Variant Effects of Non-Native Kissing-Loop Hairpin Palindromes on HIV Replication and HIV RNA Dimerization: Role of Stem−Loop B in HIV Replication and HIV RNA Dimerization†

Michael Laughrea,*,‡,§ Ni Shen,‡,§ Louis Jetté,‡ and Mark A. Wainberg‡,§,||

McGill AIDS Centre, Lady Davis Institute for Medical Research, Jewish General Hospital, and Departments of Medicine and Microbiology, McGill University, Montreal, Quebec, Canada H3T 1E2

Received July 17, 1998; Revised Manuscript Received October 8, 1998

ABSTRACT: The genome of all retroviruses consists of two identical RNAs noncovalently linked near their 5′ end. In vitro synthesized RNAs from human immunodeficiency virus type 1 (HIV-1) can form loose or tight dimers depending on whether their respective kissing-loop hairpins (nts 248−270 in HIV-1_{Lai}) bond via their hexameric autocomplementary sequences (ACS), also called palindromes, or via the ACS and stem sequences [Laughrea, M., and Jetté, L. (1996) *Biochemistry 35*, 1589−1598]. To understand the role of the ACS in HIV-1 replication and in the formation and stability of HIV-1 RNA dimers, we replaced the central CGCG261(or tetramer) of the HIV-1_{Lai} ACS by two other HIV-1 tetramers (UGCA/UGCG), four non-HIV-1 tetramers [GUAC, UUAA (respectively found in HIV-2_{Rod} and SIV_{mnd}), GGCC and AGCU (absent from HIV and SIV viruses)], or GGCG, a nonpalindromic tetramer. The infectivity of GGCC, GUAC, and UGCA viruses was unchanged or insignificantly decreased; the infectivity of AGCU and UGCG viruses was decreased by 80%; the infectivity of UUAA and GGCG viruses was decreased by 92−98%. Thus, the four non-HIV-1 palindromes yielded phenotypes ranging from wild-type to as defective as a virus bearing a nonpalindrome. Studies of in vitro synthesized HIV-1 RNAs were generally consistent with in vivo results, specifically: (i) loose dimerization of GGCC and GUAC RNAs, but not of UUAA and AGCU RNAs, was influenced by the 3′ DLS (a sequence located downstream of the 5′ splice junction) in a way expected for a wild-type ACS; (ii) the 3′ DLS strongly reduced tight dimerization of UUAA and AGCU RNAs, but not of GGCC and GUAC RNAs. We conclude that HIV-1 is sensitive to the ACS sequence without discriminating against *all* nonnative ACS: GGCC/GUAC, but not AGCU/UUAA, are good substitutes for the prevalent CGCG/UGCA native tetramers and better substitutes than the very rare UGCG native tetramer. The correlation between in vivo and in vitro results suggests that in vitro assays measure parameters of in vivo relevance. Deletion of CUCGG247 (the 5′ strand of stem−loop B) decreased the replicative capacity by more than 99.9% and metamorphosed the 3′ DLS into an inhibitor of the loose dimerization of HIV-1 RNA.

The primer binding site and the *gag* gene of the genomic RNA of human immunodeficiency virus type 1 (HIV-1)[1] are separated by 136 nucleotides (nts) extending from U200 to G335 in HIV-1_{Lai}. This 3′ half of the leader is called the L sequence (*1*). It has the potential to fold into three hairpins termed the kissing-loop domain, the 5′ splice junction hairpin, and stem−loop 3 (KLD, SD, and 3 in Figure 1). Within the HIV-1 and chimpanzee immunodeficiency virus (SIV_{cpz}) lineage, the KLD seems to be the most conserved region of the L sequence (*2*). Located in the middle of the L sequence, it encompasses a stem−loop, named the kissing-loop hairpin (nts 248−270 in Figure 1), seated on top of a short but completely conserved stem−bulge called stem−loop B (Figure 1; ref *2*).

In 49 HIV-1 and SIV_{cpz} viruses for which published L sequences are available (representing subtypes A, B, C, D, E, F, G, O, and U of HIV-1 and 2 subtypes of SIV_{cpz}), the kissing-loop hairpin is characterized by a 7 base pair stem (stem C; Figure 1) and an 8−9 nt loop (termed kissing-loop or loop C; Figure 1) containing an almost invariant hexameric autocomplementary sequence (ACS) (*2*; and references cited therein), also called palindrome. The palindrome is considered to be the dimerization initiation site (DIS) of HIV-1 genomic RNA.

† This work was supported by a grant (MT-12312) from the Medical Research Council of Canada to M.L.

* To whom correspondence should be addressed at the Lady Davis Institute for Medical Research, 3755 Cote Ste. Catherine Rd., Montreal, Quebec, Canada H3T 1E2. Telephone: (514)340-8260. FAX: (514)340-7502.

‡ Sir Mortimer B. Davis−Jewish General Hospital.

§ Department of Medicine, McGill University.

|| Department of Microbiology, McGill University.

[1] Abbreviations: HIV-1, human immunodeficiency virus type 1; SIV, simian immunodeficiency virus; nt, nucleotide; KLD, kissing-loop domain; ACS (or palindrome), 6 nt long autocomplementary sequence located in the loop of the kissing-loop hairpin; tetramer, the central 4 nts of the ACS; 3′ DLS, RNA sequence located downstream of the 5′ splice junction, starting at A296 and ending at G508; $TCID_{50}$, 50% tissue infective dose; T_d, apparent dissociation temperature; SIV_{cpz}, chimpanzee immunodeficiency virus; SIV_{mnd}, mandrill immunodeficiency virus; NNNN virus or NNNN RNA, HIV-1_{Lai} virus or RNA whose CGCG261 tetramer has been replaced by NNNN, where N could be any of the 4 canonical nts; CAp24, capsid protein; SEM, standard error of the mean.

10.1021/bi981728j CCC: $18.00
Published on Web 12/05/1998

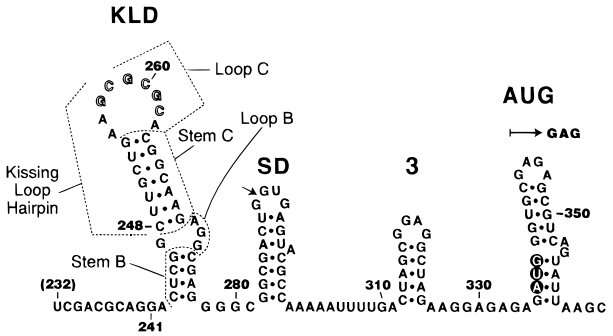

FIGURE 1: Secondary structure model for the HIV-1_{Lai} L sequence. The cleavage site within the 5′ major splice donor is marked by an arrow within the SD hairpin. The AUG initiation codon of the gag gene is highlighted and somewhat arbitrarily presented as hydrogen-bonded in the interest of a compact figure. This model is based on published stucture probing and/or phylogenetic data (*2*, and references cited therein). The nucleotides of the GCGCGC262 palindrome are highlighted.

Mutations in the kissing-loop hairpin have recently been shown to reduce viral infectivity (*2, 3*), genomic RNA packaging (*2*−*6*), genomic RNA dimerization (*2, 5, 7*), proviral DNA transcription (*2, 8*), and proviral DNA synthesis (*3, 9*).

In the kissing-loop model of HIV-1 genome dimerization (*10*−*12*), HIV-1 RNA dimerization is initiated by base-pairing between the ACS of one RNA monomer and that of an adjacent monomer (Figure 1). HIV-1 RNA can form two types of dimers, termed loose and tight dimers apparently depending on whether the kissing-loop hairpins interact via their ACS only or, more completely, via their ACS and stem C sequences (*12*−*15*). Loose HIV-1 RNA dimers cannot resist electrophoresis in buffer TBE_2 at 27 °C; tight dimers are operationally defined as HIV-1 RNA dimers which can withstand electrophoresis in TBE_2 at 27 °C (*13*; see below). Loose dimers of HIV-1_{Mal} RNAs, but not of HIV-1_{Lai} RNAs, are stabilized by the 3′ DLS, a sequence located within the 296−508 region, i.e., downstream of the 5′ splice junction (*12, 16*).

Out of 49 HIV-1/SIV_{cpz} loop C sequences, the ACS GCGCGC262 is found in 27 sequences (SIV_{cpzant} and all HIV-1 subtypes B, D, and F); GUGCAC is found in 21 (SIV_{cpzgab}, all HIV-1 subtypes C, E, G, O, U, and 1 HIV-1 subtype A); and GUGCGC is found in HIV-1_{Ibng}, an ill-documented subtype A virus. Given this nonrandom outcome [only 3 different native ACS uncovered out of 41 theoretically strong ACS candidates (*17*)], a key property of HIV-1 genomic RNA might be exquisitely sensitive to the exact shape of the kissing-loop hairpin. To validate this idea, the ACS of HIV-1_{Lai} was serially replaced by four non-HIV-1 ACS, the two other native ACS, or GGGCGC, a nonpalindrome. First, we studied the effect of these various ACS on HIV-1 replication. Second, we characterized the ACS−3′ DLS interplay in the formation and thermostability of loose and tight HIV-1 RNA dimers. Our results indicate that HIV-1 replication and HIV-1 RNA dimerization are sensitive to the ACS sequence, but not to the point of discriminating against all non-wild-type palindromes. They further document two forms of communication between the ACS and the 3′ DLS.

Finally, a secondary goal of this paper was to initiate experiments designed to estimate the importance of stem−loop B in HIV-1 replication, genomic RNA encapsidation, and HIV-1 RNA dimerization. We show that stem−loop B is crucial for viral replication and that destroying the 5′ strand of stem−loop B alters the function of the 3′ DLS.

MATERIALS AND METHODS

Buffers and Glassware. Buffer L (*10*): 50 mM sodium cacodylate, pH 7.5, 40 mM KCl, and 0.1 mM $MgCl_2$. Buffer H (*10*): 50 mM sodium cacodylate, pH 7.5, 300 mM KCl, and 5 mM $MgCl_2$. TBE_2 and TB (*18*): 89 mM Tris, 89 mM borate, and respectively 2 mM and no EDTA. All glassware used in this paper was cooked overnight, and all H_2O used for in vitro experiments was diethyl pyrocarbonate treated.

Plasmid Construction. Standard techniques were used for molecular cloning (*19*), and nucleotide positions are those of the HIV-1_{Lai} genomic RNA. Plasmid pSVC21.BH10 encodes an infectious HIV-1_{Lai} molecular clone derived from the IIIB strain of HIV-1. The plasmid also carries an SV40 origin of replication for expression in COS cells, which are African green monkey kidney cells transformed by simian virus 40 (*2*).

The kissing-loop domain of pSVC21.BH10 was altered as previously described (*2*), using cassette mutagenesis of plasmid pBH and transfer of the mutated region into pSVC21.BH10. To prepare pBH, pSVC21.BH10 was cleaved with *Bgl*II and *Apa*I to extract the 18−1556 region of the HIV-1 genome. This fragment was then ligated into pBluescript KS^- to have the 18−1556 region cloned in front of a strong T7 RNA polymerase promotor. This was followed by digestion with *Nar*I and *Bss*HII to create a gap between nts 187 and 261. We then ligated various ∼70 bp duplexes into this gap. Nine mutants were thus prepared. The seven ACS mutants were respectively termed GGCC, GUAC, UGCA, UGCG, UUAA, AGCU, and GGCG (CGCG261 respectively replaced by GGCC, GUAC, UGCA, UGCG, UUAA, AGCU, or GGCG). The two deletion mutants, termed Δ243−247 and Δ248−256, are self-explanatory. In the first, the 5′ strand of stem−loop B was deleted; in the second, the 5′ strand of stem C plus AA256 was deleted (Figure 1). All constructs were sequenced to verify that the correct mutations had been achieved.

Transfections and Virus Preparation (2). Ten to thirty 100 by 20 mm tissue culture dishes of COS-7 cells were transfected with mutant plasmids pSVC21GGCC, GUAC, etc. by the calcium phosphate method. In each transfection experiment, an equal number of tissue culture dishes were concurrently transfected with plasmid pSVC21.BH10 to produce the control BH10 virus to which mutants were compared. Viruses were isolated from the DMEM/fetal calf serum cell culture supernatant (7 mL/dish) at 63 h posttransfection. The supernatant was centrifuged in a GS-6R rotor at 3000 rpm for 15 min and passed through a 0.22 μm cellulose acetate filter (Corning). This clarified COS-7 culture supernatant fluid was centrifuged in a Ti45 rotor at 35 000 rpm for 1 h at 4 °C. The pellet was dissolved in phosphate-buffered saline (*19*) and centrifuged over 6 mL of 20% sucrose in phosphate-buffered saline, using an SW41 rotor (26 500 rpm, 1 h 55 min, 4 °C). The average virus yield was 4×10^9 virions per 10 Petri dishes (assuming 2000 capsid proteins per virion).

Infectivity Assay. The number of 50% tissue culture infective doses ($TCID_{50}$) contained in a mutant and a wild-

type viral preparation was measured in two 96-well flat bottomed plates as previously described (*2*). To do each experiment in octuplicate, each of the eight wells in the second vertical row contained 12.8 μL of clarified COS-7 culture supernatant fluid in a final volume of 200 μL of R-20 medium containing 2×10^4 MT4 target cells. The third to eleventh vertical rows contained serial dilutions of the virus (from 4^{-1} to 4^{-9} dilutions). Culture fluids were replaced at day 4 after infection. Cytopathic effects (multinucleated giant cell formation−syncytium formation with ballooning cytoplasm) were assessed at days 4 and 7 after infection, and the number of $TCID_{50}$ was calculated by the method of Reed and Muench (*2*). One $TCID_{50}$ is the lowest amount of virus able to infect 50% of cell cultures at day 7 as measured by visible cytopathic effects. Viral infectious titers are reported as number of $TCID_{50}$/ng of capsid protein ± the standard error of the mean (SEM).

Physical Virus Titer. The physical virus titer was determined as described previously (*2*), by estimating the amount of capsid protein (CAp24) in purified viruses or in clarified COS-7 culture supernatant fluid. CAp24 was estimated using a p24 enzyme-linked immunosorbent assay (ELISA) detection kit (Abbott Laboratories) according to the manufacturer's recommendations.

Isolation of HIV-1 Genomic RNA. Viruses were disrupted in 0.5−1 mL of sterile lysis buffer consisting of 50 mM Tris (pH 7.4), 10 mM EDTA, 1% sodium dodecyl sulfate (SDS), 50 mM NaCl, 50 μg of yeast tRNA/mL, and 100 μg of proteinase K/mL (*20*). Resuspended pellets were incubated at 37 °C for 1 h 10 min and then extracted 3 times with an equal volume of buffer-saturated phenol−chloroform−isoamyl alcohol (25:24:1, pH 7.5). The aqueous phase, containing the viral RNA, was precipitated in 70% ethanol at −80 °C, using 0.3 M sodium acetate (pH 5.2). Viral RNA pelleted from ethanol suspension was dissolved in a buffer containing 10 mM Tris (pH 7.5), 1 mM EDTA.

Genomic RNA Packaging Assay. The amount of genomic RNA per virus was quantitated by hybridization with radioactive antisense RNA 636−296, as described previously (*2*). Genomic RNAs isolated from equivalent amounts of viruses (on the basis of CAp24 content) were vacuum-transferred to a Hybond N^+ nylon membrane sandwiched within a Hybri-Dot filtration manifold. After drying, cross-linking, and prehybridization, the nylon membrane was hybridized overnight to approximately 10^7 cpm of antisense RNA 636−296. This was followed by 3 washes and autoradiography. The autoradiograms were scanned with a Supervista S-12 UMAX densitometer, and to confirm the scans, the radioactivity present in each individual spot of the nylon membrane was scintillation-counted.

In Vitro RNA Synthesis and Recovery. Prior to T7 RNA polymerase transcription, plasmids pBH, pBHGGCC, pBHGUAC, pBHUGCA, pBHUGCG, pBHUUAA, pBHAGCU, pBHGGCG, pBHΔ243−247, and pBHΔ248−256 were cleaved with *Rsa*I and *Acc*I to obtain RNAs starting at C18 and respectively ending at U295 or G508. Some of the plasmids were also cleaved with *Hae*III or *Dra*I to obtain RNAs respectively ending at G401 or U790. Transcription and RNA recovery were done using the MEGAscript kit of Ambion (*17*).

In Vitro Dimerization of HIV-1 RNAs. The dimerization procedures were described previously (*12, 13, 17*). A 500 ng to 1 μg amount of RNA dissolved in 8 μL of water was heated for 2 min at 92 °C and chilled for 2 min on ice. For preparation of loose dimers, 2 μL of 5× concentrated buffer L or H was added, and the samples were incubated for 30 min at 30 °C in buffer L or in buffer H. For preparation of tight dimers (*13*), 2 μL of 5× concentrated buffer L or H was added, and the samples were preincubated 30 min at 0 °C and incubated for 10 min at the indicated temperatures (which ranged from 43 to 70 °C). The samples were loaded on 2.5% agarose gels after addition of 2 μL of loading buffer containing glycerol. Electrophoresis (4−5 W, 70−100 min) proceeded at 4 °C in buffer TB or at 27 °C in buffer TBE_2, as indicated (*17*). After electrophoresis, the gels were stained, and the percentage of dimerization was estimated by scanning the photographic negatives with a Supervista S-12 UMAX densitometer (*12, 17*). To measure the apparent dissociation temperature (T_d) of the loose dimers, four or five different 10 μL samples of the same dimeric RNA were simultaneously postincubated for 10 min at four or five different temperatures (e.g., 34, 37, 41, 45, and 49 °C for RNAs with low T_ds, or 45, 49, 53, 57, and 61 °C for RNAs with high T_ds, etc.). These RNA samples were next loaded on the gel without delay and with the voltage on (*17*).

RESULTS

Sequence Dependence of HIV-1 Replication. To produce HIV-1 viruses mutated within the central CGCG261 (or tetramer) of the ACS or bearing deletions within the KLD, COS-7 cells were transfected in parallel with equal amounts of control plasmid pSVC21.BH10 and mutant plasmids such as pSVC21GGCC, GUAC, UGCA, AGCU, UGCG, UUAA, *G*GCG, Δ243−247, and Δ248−256. [In pSVC21GGCC, CGCG261 has been replaced by GGCC; in pSVC21Δ243−247, CUCGG247 has been deleted; mutatis mutandis for the other plasmids; nts differing from $HIV\text{-}1_{Lai}$ and $HIV\text{-}1_{Mal}$ (subtype U) nts are underlined.] Comparable amounts of viruses (i.e., ±50%) were produced at 63 h posttransfection, as measured by the number of capsid proteins (CAp24) present in the culture supernatant and in the purified virus fraction (not shown). Thus, the mutations had no major effect on HIV-1 genomic DNA transcription and virus production. To assess the quality of the virus produced, the number of $TCID_{50}$ contained in two to four independent preparations of mutant viruses was measured. Each experiment was performed in octuplicate (Materials and Methods). Since each one involved serial dilutions, the results are best presented in logarithmic form [Table 1; for comparison, mutants ACS^- ($HIV\text{-}1_{Lai}$ containing 5 nt substitutions within the 254−261 sequence) and Δ248−261 (*2*) are also tabulated]. Though the mutants display as a group an almost continuous range of replicative capacity (Table 1), it is possible to divide them into five classes. (a) GGCC, GUAC, and UGCA viruses replicated at near-wild-type levels (on average 37% fewer $TCID_{50}$/unit CAp24 than $HIV\text{-}1_{Lai}$, an insignificant difference). (b) AGCU and UGCG viruses replicated moderately slower than wild type (on average 80% fewer $TCID_{50}$/CAp24). (c) UUAA and GGCG viruses were clearly abnormal (∼96% fewer $TCID_{50}$/CAp24 than wild type). (d) ACS^-. (e) Highly defective viruses: Δ243−247 and Δ248−256 viruses (respectively 99.96 and 99.92% fewer $TCID_{50}$/CAp24 than wild type) were crippled to roughly the same extent as Δ248−261 viruses (which had lost the palindrome

Table 1: Infectious Titers of HIV-1_{Lai} Relative to Those of Mutant Viruses[a]

mutant[b]	log (BH10/mutant ratio)	no. of independent infectivity tests	class/qualitative assessment	range (BH10/mutant)
UGCA	0.15 ± 0.25	2	a/wild-type-like	0.8−2.5
GUAC	0.1 ± 0.2	2	a/wild-type-like	0.8−2.0
GGCC	0.4 ± 0.2	3	a/wild-type-like	1.6−4
UGCG	0.65 ± 0.3	2	b/borderline	2.2−9
AGCU	0.75 ± 0.25	3	b/borderline	3−10
UUAA	1.35 ± 0.25	3	c/abnormal	13−40
GGCG	1.45 ± 0.25	3	c/abnormal	16−50
ACS$^-$	2.3 ± 0.15[c]	2	d/defective	140−280
Δ248−256	3.1 ± 0.25	4	e/highly defective	700−2200
Δ243−247	3.45 ± 0.35	3	e/highly defective	1300−6300
Δ248−261	3.65 ± 0.25[c]	3	e/highly defective	2500−8000

[a] In each infectivity test, the number of $TCID_{50}$ per nanogram of capsid protein (CAp24) was determined in octuplicate by using 4-fold serial dilutions against a control BH10 population (see Materials and Methods). The data shown were determined by the method of Reed and Muench. The SEMs are also shown. [b] In palindrome mutants, only the central 4 nts of the palindrome are indicated (the HIV-1_{Lai} sequence is CGCG261). [c] From Laughrea et al. (*2*). In ACS$^-$, GAAGCGCG261 was replaced by AGAUCACU261.

Table 2: Some Mutant Genomic RNAs Are Poorly Packaged into Virions

mutant[a]	rel encapsidation efficiency[b]	no. of independent expt
GGCC	0.8 ± 0.25	2
GUAC	0.8 ± 0.25	2
UGCA	1.1 ± 0.25	4
UGCG	1.4 ± 0.4	2
UUAA	1.1 ± 0.15	2
AGCU	0.5 ± 0.25	4
GGCG	0.6 ± 0.20	4
Δ243−247	0.6 ± 0.10	2
Δ248−256	0.7 ± 0.25	3

[a] Mutants defined as in Table 1. [b] The relative encapsidation efficiency is defined as: [number of mutant genomic RNAs per unit of CAp24] divided by [number of wild-type genomic RNAs per unit of CAp24]. The SEM is shown.

and the 5′ strand of stem C). Thus, the four non-HIV-1 tetramers[2] yielded infectivities ranging from wild-type (GGCC and GUAC) to borderline (AGCU) and abnormal (UUAA), but none were as damaging as the deletion of the 5′ strand of stem−loop B. This is not necessarily surprising since Δ243−247 should strongly disturb at least nine nt positions whereas the most deleterious tetramer mutation (GGCG) might disturb only one nt position (Figure 1).

Sequence Dependence of Genomic RNA Encapsidation. Viral genomic RNA was extracted from equivalent amounts of virus, as determined by an antigen-capture assay to detect CAp24. This virion RNA was then identified by dot-blot hybridization using a ^{35}S-labeled HIV-1 riboprobe (Materials and Methods). The HIV-1 RNA in each spot was quantitated by scanning the autoradiograms and scintillation counting the individual spots (*2*). Table 2 shows that most mutations had no effect on genomic RNA packaging. Exceptions were the Δ243−247 mutant and two tetramer mutants: GGCG (nonpalindromic) and AGCU.

Loose dimers of AGCU and UUAA RNAs are thermolabile because the 3′ DLS does not stabilize them. Loose dimers of GUAC, UGCA, and UGCG RNAs are stabilized by the 3′ DLS. Loose dimers of GGCC and HIV-1_{Lai} RNAs are thermoresistant even in the absence of the 3′ DLS, thereby masking the putative contribution of the 3′ DLS. Plasmid pBH contains the 18−1556 region of the HIV-1_{Lai} genome cloned in front of a strong T7 RNA polymerase promotor (*2*). We replaced its CGCG261 tetramer (Figure 1) by GGCC, GUAC, UGCA, UGCG, UUAA, AGCU, or GGCG (Materials and Methods), to yield plasmids pBHGGCC, GUAC, UGCA, UGCG, UUAA, AGCU, and GGCG. In pBHΔ243−247 and Δ248−256, CUCGG247 and CUUGCUGAA256 were respectively deleted. Prior to transcription, the plasmids were cleaved with *Rsa*I or *Acc*I to yield RNAs ending at U295 or G508. To produce loose dimers, the RNAs were incubated 30 min at 30 °C in buffer H (a high ionic strength buffer containing 350 mM monovalent cations and 5 mM Mg^{2+}) or in buffer L (a low ionic strength buffer containing 90 mM monovalent cations and 0.1 mM Mg^{2+}) prior to electrophoresis at 4 °C on an agarose gel containing buffer TB (*12*, *17*).

The dimerization yields of RNAs bearing mutant tetramers are shown in Table 3A. Consistent with the infectivity results and the kissing-loop model, UUAA and GGCG RNAs dimerized very poorly. The other RNAs dimerized almost normally (i.e., reached 50−60% of HIV-1_{Lai} levels on average) except that GUAC RNA, when deprived of the 3′ DLS, dimerized at least as poorly as UUAA RNA. Thus, the 3′ DLS stabilizes GUAC RNA dimers or facilitates the folding of its kissing-loop into a more productive configuration.[3]

To measure the T_d of the dimeric RNAs, loose dimers were prepared by a 30 min incubation at 30 °C and postincubated for 10 min at either 34, 37, 41, 45, 49, 53, 57, or 61 °C prior to electrophoresis (*12*, *17*). T_d[4] was scored as the temperature at which percent dimerization was half-maximal. The T_ds of RNAs bearing mutant tetramers are shown in Table 4A. RNAs truncated at G508 and incubated in buffer H (second column of Table 4A) can be divided into three groups: GGCC, GUAC, and HIV-1_{Lai} RNAs had a high T_d (≥55 °C); UGCA and UGCG RNAs had an intermediate T_d (51 °C); UUAA and AGCU RNAs had a low T_d (43−47 °C). [GGCG RNA, which hardly dimerized (Table 3A), was

[2] The GGCC and AGCU tetramers are absent from the kissing-loop hairpins of all human and simian immunodeficiency viruses so far sequenced; the GUAC and UUAA tetramers are respectively found in the putative kissing-loop hairpins of HIV-2_{Rod} and SIV_{mnd} (*2*, *22*).

[3] A similar 3′ DLS-promoted increase in dimer yield was found in an HIV-1_{Mal} RNA mutated to possess a UCGA tetramer (*26*).

Table 3: Dimerization Yield in Buffers H or L of HIV-1_{Lai} and Mutant HIV_{Lai} RNAs Ending at G508 or U295

	% dimerization of RNAs[a]				
	in buffer H and ending at		in buffer L and ending at		
mutation	G508	U295	G508	U295	$\Delta G°(37)$ (kcal/mol)[b]
(A) Wild-Type RNA (CGCG) and RNAs Having CGCG261 Replaced by the First 7 Indicated Sequences					
UUAA	**14 ± 4**	**18 ± 2**	<**3**	<**3**	−3.3
GGCG	**8 ± 3**	nd[e]	nd	nd	−
GUAC	60 ± 11	**12 ± 2.3**	55 ± 8	<**3**	−7.3
GGCC	40 ± 11	55 ± 4	29 ± 9	47 ± 4	−11.2
AGCU	∼40[c]	∼30[c]	33 ± 12	38 ± 3	−7.6
UGCA	∼40[c]	∼30[c]	53 ± 14	35 ± 6	−7.4
UGCG	∼40[c]	∼30[c]	43 ± 7	47 ± 5	−6.2
CGCG	>80[c,d]	>80[c,d]	60 ± 16	69 ± 14	−10.4
(B) RNAs Where CUCGG247 or CUUGCUGA256 Was Deleted					
Δ243−247	35 ± 7	46 ± 4	6 ± 3	36 ± 11	−
Δ248−256	7 ± 2	nd	nd	nd	

[a] The RNAs were dimerized by incubation at 30 °C in buffers H or L and were asssayed by agarose gel electrophoresis in buffer TB at 4 °C (Materials and Methods). RNAs which dimerized poorly are in boldface type. SEMs of typically four measurements are indicated. [b] Calculated $\Delta G°(37)$ (27−29) of duplexes formed in 1 M NaCl by hexanucleotides having the sequence of the respective palindromes. [c] From Laughrea and Jetté (*17*). [d] From Laughrea and Jetté (*12*). [e] nd: not done.

Table 4: Apparent Dissociation Temperature (T_d) in Buffers H and L of HIV-1_{Lai} and Mutant HIV-1_{Lai} RNAs Ending at G508 or U295

	T_d (°C) of RNAs			
	in buffer H and ending at		in buffer L and ending at	
mutation	G508	U295	G508	U295
(A) Wild-Type RNA (CGCG) and RNAs Having CGCG261 Replaced by Indicated Sequences				
GGCC	60 ± 3[a]	58	45 ± 4	45.5
GUAC	60 ± 3	51 ± 5	50.5	−
CGCG	55[b]	55[b]	46[b]	46[b]
UGCA	51[c]	42.5[c]	42.5	40.5
UGCG	51.5[c]	42.5[c]	![d]	![d]
UUAA	46	47	−	−
AGCU	43.5[c]	43[c]	41 ± 5	48 ± 4
GGCG	?[e]	nd[f]	nd	nd
(B) RNAs Where CUCGG247 Was Deleted				
Δ243−247	55 ± 5	55 ± 6	42.5	48 ± 4
Δ248−256	nd	nd	nd	nd

[a] Margins of errors (indicated when larger than 2 °C) are standard deviations of at least three T_d numbers. The 18 standard deviations which were not spelled out were 1.5 °C on average. [b] From Laughrea and Jetté (*12*). [c] From Laughrea and Jetté (*17*). [d] Not tabulated because the margins of errors were impractibly high. The T_ds appeared to be within the 40−55 °C range. [e] T_d was measured in one experiment, and the result was 40 °C. [f] nd: not done.

not investigated.] The third column indicates that GUAC, UGCA, and UGCG RNAs were destabilized by the loss of the 3′ DLS (T_d reduced by ∼9 °C), while AGCU, UUAA, GGCC, and HIV-1_{Lai} RNAs were not. Thus, with or without 3′ DLS, GGCC and HIV-1_{Lai} RNAs were thermostable, while AGCU and UUAA RNAs were unstable. GGCC and HIV-1_{Lai} RNAs are unrevealing because their high T_d presumably masks any putative contribution from the 3′ DLS (*17*). The inability of the 3′ DLS to stabilize AGCU and UUAA RNAs shows that the 3′ DLS of these RNAs misinteracted (or failed to interact) with what was its site of action in GUAC, UGCA, and UGCG RNAs. Note that the AGCU and UUAA tetramers are absent from the kissing-loop of HIV and SIV_{cpz} viruses. Results in buffer L (fourth and fifth columns of Table 4A) were generally consistent with those in buffer H, except that UGCA RNA was not stabilized by the 3′ DLS, as if 3′ DLS function was more Mg^{2+} dependent in the presence of UGCA than in the presence of GUAC,[5] or as if our gel assays overestimated T_ds that should have been <40 °C.

In short, at high ionic strength, the 3′ DLS *did not stabilize* AGCU and UUAA RNA dimers (length-independent T_d of ∼45 °C), stabilized UGCA, UGCG, and GUAC RNA dimers (T_d of ∼54 °C with the 3′ DLS and ∼45 °C without), and made perhaps a concealed contribution to the stability of GGCC and HIV-1_{Lai} RNA dimers (length-independent T_d of ∼57 °C).

[4] Out of 29 published thermal analyses of retroviral dimeric RNAs (18 on HIV-1 RNAs), 28 have involved nondenaturing gel electrophoresis and 1 has involved glycerol gradient centrifugation, but none has involved alternative methods to separate monomeric from dimeric RNAs (*17*, and references cited therein; *26*). We are aware that T_ds obtained by such an economical technique cannot be regarded as absolute because the data are not taken at equilibrium and the incubation buffer usually differs from the electrophoresis buffer. However, such T_ds are useful when the goal is to compare RNAs of different sequences and to compare our results to previous thermal analyses of retroviral RNA dimerization. Thus, the meaningful results of the present T_d study are not so much the exact numerical T_d values obtained but *the sequence dependence of these values*.

[5] Consistent with the idea of a Mg^{2+} sensitivity of the 3′ DLS function in the 0.1 mM range, UGCG RNA dimers had reasonable but highly variable T_ds in buffer L (respective standard deviations of 11 and 8 °C with RNAs 18−508 and 18−295).

Poor Loose Dimerization of Δ243−247 RNA Is Mainly Due to 3′ DLS Misinteraction with the Kissing-Loop Hairpin. To investigate if regions other than the palindrome might influence dimerization and 3′ DLS function, we studied Δ243−247 RNAs ending at U295 and G508. Δ243−247 RNA was, in buffer L, 6 times more dimeric when it ended at U295 than when it ended at G508, as if the 3′ DLS misinteracted with the kissing-loop hairpin in the absence of stem−loop B (Table 3B). However, once dimerized, Δ243−247 RNA appeared as thermostable as HIV-1_{Lai} RNA (Table 4B). These findings have two implications: the 3′ DLS might trap Δ243−247 RNA ending at G508 in a conformation which partially secludes the palindrome at 30−37 °C; stem−loop B makes at best a concealed contribution to the T_d of dimeric HIV-1_{Lai} RNA.

To learn if it was the 5′ or 3′ half of the 3′ DLS which interfered with Δ243−247 RNA dimerization, we tried to dimerize RNAs ending at G401: Δ243−247 RNA was *monomeric* (<5% dimeric) in buffer L *and in buffer H* (not shown), while HIV-1_{Lai} RNA was, as expected (*10*, *13*), respectively ∼65% and >80% dimeric. Thus, the interference came from the 296−401 sequence. Finally, Δ243−247 RNA ending at U790 behaved like Δ243−247 RNA ending at G508 (not shown), confirming that the 5′ strand of stem−loop B prevents the 3′ DLS from becoming an inhibitor of dimerization, and opening the possibility that this holds in longer RNAs.

Finally, even without the 3′ DLS, the dimerization yield of Δ243−247 RNA was ∼50% lower than that of HIV-1_{Lai} RNA (Table 3). Thus, with or without the 3′ DLS, stem−loop B protects the palindrome from partial seclusion at 30−37 °C.

Tight Dimers of UUAA and AGCU RNAs Are Inefficiently Formed Due to 3′ DLS Interference. Formation of tight HIV-1 RNA dimers require incubation at 30−37 °C in the presence of NCp7 (*15*) or incubation at 45−65 °C in the absence of NCp7 (*13*, *14*). This suggests that tight dimerization of HIV-1 RNA might play a physiological role. [This role might be connected to mature HIV-1 genomic RNA having a higher T_d than immature genomic RNA (*13*, *20*).] If this role is important, then all wild-type HIV-1 RNAs should be able to form tight dimers at 37 °C (in the presence of NCp7) or at >45 °C (in the absence of NCp7), no matter their subtype of origin, whereas judiciously chosen KLD mutants might not.

Accordingly, we tested if RNAs truncated at G508 could form tight dimers at temperatures ranging from 46 to 69 °C in buffer H (Figure 2) and from 43 to 61 °C in buffer L (Figure 3). As assessed by electrophoresis in buffer TBE_2 at 27 °C, GGCC, GUAC, and Δ243−247 RNAs formed tight dimers in buffer H as efficiently as UGCA, UGCG, and HIV-1_{Lai} RNAs (Figure 2: compare ○, □, and △ to thick continuous line); UUAA RNA did not (●). UUAA RNA tight-dimerized as poorly as AGCU RNA (dotted line) and 5-fold more poorly than the other RNAs. This difference was as detectable at 55 °C as at higher temperature, suggesting physiological significance. An analogous picture emerged in buffer L (Figure 3). At 52−58 °C, the yield of UUAA RNA tight dimers was 2.5−3-fold lower than that of Δ243−247, GGCC, UGCA, UGCG, and HIV-1_{Lai} RNAs (compare ● to △, ○, and thick continuous line), and 2-fold lower than that of GUAC RNA. In short, UUAA and AGCU

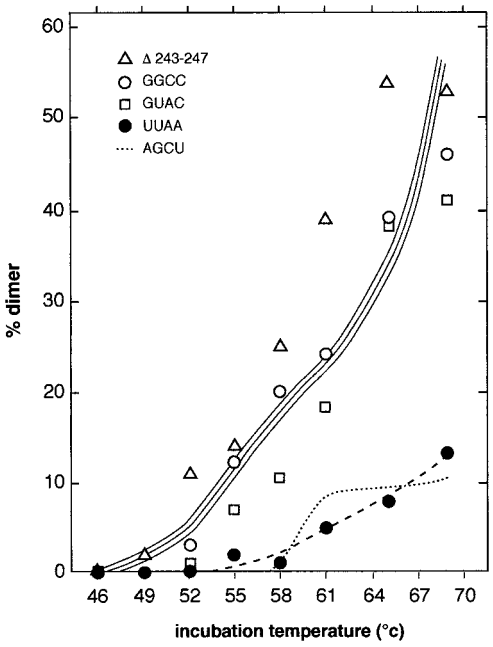

FIGURE 2: Net tight dimerization of HIV-1 RNAs ending at G508 as a function of incubation temperature. Incubation in buffer H was for 10 min at the indicated temperatures prior to agarose gel electrophoresis in TBE_2 at 27 °C (Materials and Methods). To clarify presentation and interpretation, a 0−9% tight dimeric RNA background has been subtracted. Background is defined for each temperature as the average percent tight dimers observed with GGCG, ACS^-, and Δ248−261 RNAs: 3% at 49 °C in buffer L, 6% at 52 and 55 °C in buffer L, 3% at 58 °C in buffers L and H, 9% at 61 and 65 °C in buffer H, and <3% at other incubation conditions (*17*). (△) Δ243−247 RNA; (○) GGCC RNA; (□) GUAC RNA; (●) UUAA RNA; thick continuous line, UGCA, UGCG, and HIV-1_{Lai} RNAs, three RNAs which had undistinghishable tight dimerization yields (*17*); dotted line, AGCU RNA (*17*). Each data point represents the average of 2−5 experiments.

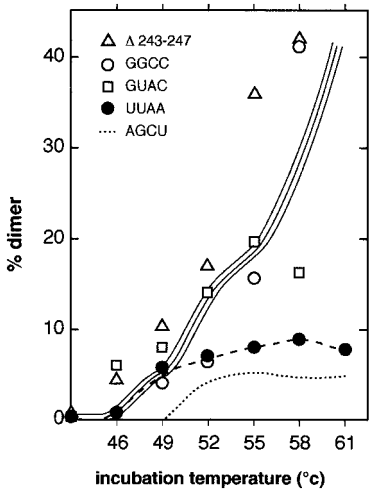

FIGURE 3: Net tight dimerization of HIV-1 RNAs in buffer L. Procedures and presentation otherwise as in Figure 2.

RNAs behaved similarly (compare ● to dotted line), except at 49 °C in buffer L; however, little weight can be attached to the 49 °C data because all relevant RNAs tight-dimerized poorly at that temperature.

The tight dimerization yield of AGCU RNA was reduced 5-fold by the 3′ DLS while that of UGCA, UGCG, and HIV-1_{Lai} RNAs was unaffected or inhibited a nonsignificant ≤2-fold (*17*). To probe this apparent differentiation between native and non-native tetramer, the effect of removing the

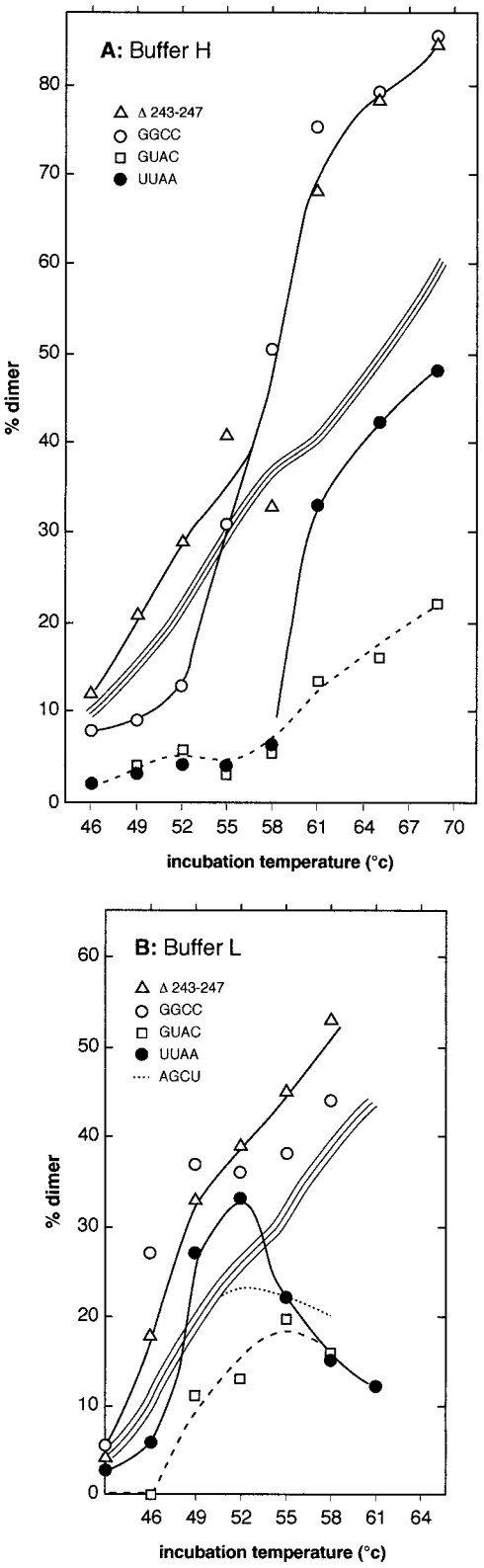

FIGURE 4: Tight dimerization of HIV-1 RNAs ending at U295 as a function of buffer and incubation temperature. Panel A, buffer H; panel B, buffer L. Procedures and presentation as in Figure 3, except that the dashed line highlights GUAC RNA. In both panels, the dotted line (AGCU RNA) is not displayed when it overlaps with the thick continuous line (see ref *17* for details).

3′ DLS on the tight dimerization of the other RNAs was investigated (Figure 4). As in ref *17*, we divided the data of Figures 2 and 3 by the cognate data of Figure 4A,B and categorized the results as wild-type-like (tight dimerization uninhibited or inhibited ≤2-fold by the 3′ DLS) or abnormal (tight dimerization inhibited >2-fold). We found that Δ243−247 and GUAC RNAs were wild-type-like, that GGCC RNA was borderline, and that UUAA RNA was abnormal, like AGCU RNA. Specifically, the effect of the 296−508 region was as follows. (a) Δ243−247 RNA: yield decreased by 45% (buffers L and H); (b) GUAC RNA: yield unchanged (buffer L) or doubled (buffer H); (c) GGCC RNA: yield decreased by ∼60% (buffer H) or by a variable amount averaging ∼50% (buffer L); (d) UUAA RNA: yield reduced 5-fold in buffer H (● of Figure 2 divided by ● of Figure 4A; temperatures where both dimerization yields were <10% were not considered), 5-fold in buffer L at 49−52 °C, and 2.5−3-fold in buffer L at 55 °C (● of Figure 3 divided by ● of Figure 4B).

In sum, tight dimerization was significantly inhibited only in UUAA and AGCU RNAs. Why? Because the UUAA and AGCU tetramers (but not the Δ243−247 deletion) misdirected the 3′ DLS toward a negative impact on tight dimerization.

DISCUSSION

This paper sheds new light on the function of the palindrome and stem−loop B of the HIV-1_{Lai} KLD, as well as on the interplay between the 3′ DLS and the KLD.

On the Palindrome. Our results indicate that HIV-1 adopts some *middle-of-the-road* palindromic selectivity. Namely, according to five functional criteria (infectivity, genomic RNA packaging, yield of loose RNA dimers, T_d of loose dimers, and yield of tight RNA dimers), the GGCC261 and GUAC261 tetramers yielded HIV-1 viruses and RNAs functionally equivalent to viruses and RNAs bearing the CGCG/UGCA tetramer (Figure 1); in contrast, AGCU and UUAA were below normal according to at least four of these criteria (Table 5). We conclude that HIV-1 replication and HIV-1 RNA dimerization are sensitive to the ACS sequence, but not to the point of rejecting all non-wild-type palindromes.

Several lessons are learned from our experiments. First, the good correlation observed between viral replication and in vitro RNA dimerization (Table 5) suggests that our in vitro assays are physiologically relevant. Second, there is no need for a central GC or a purine/pyrimidine alternance in a functional palindrome, because the GGUACC and GGGCCC palindromes yielded wild-type phenotypes. Third, a palindrome having a high G/C content and a central GC is not necessarily functional: GAGCUC yielded an abnormal phenotype. Fourth, the palindrome influences RNA dimerization directly and also indirectly, e.g., by channeling the 3′ DLS toward a positive role in loose dimerization (Tables 3 and 4) and away from a negative role in tight dimerization (Figures 2−4). Fifth, UGCA261, though never found in subtype B, D, and F viruses, could substitute for the tetramer of HIV-1_{Lai} (subtype B); however, UGCG261 was a borderline substitute, consistent with its rarity in the wild[6] (see below). The present paper rules out previously aired ideas such as (a) palindromes might need a central GC or alternating purines and pyrimidines (e.g., ref *21*) or (b) only

[6] It is not known if GUGCGC is an excellent palindrome within its native sequence context, i.e., that of subtype A HIV-1_{Ibng}. Thus, its "native" status can be questioned.

Table 5: In Vivo and in Vitro Phenotypes of HIV-1 Viruses and RNAs Bearing Mutant Palindromes: Summary of Tables 1−4 and Figures 2−4

mutation (nts 258−261)	infectivity	genomic RNA packaging	loose dimer yield	T_d	tight dimer yield
GGCC	∼wt[a]	∼wt	∼wt	∼wt	∼wt
GUAC	∼wt	∼wt	∼wt	∼wt	∼wt
UGCA	∼wt	∼wt	∼wt	∼wt	∼wt
UGCG	borderline	∼wt	∼wt	∼wt	∼wt
AGCU	borderline	low	∼wt	low	low
UUAA	abnormal	∼wt	very low	low	low
GGCG	abnormal	low	very low	−	very low

[a] ∼wt means wild-type-like.

a few different palindromes might allow normal HIV-1 function (e.g., ref *17*).

Putting our results together, the following rules for constructing a functional KLD palindrome can be proposed. First, a central GC (or even a central GC combined to a ≥66% G/C-rich content) is neither necessary nor sufficient. Second, a ≥66% G/C-rich content might be necessary (GUUAAC, an average G/C-poor palindrome[7] was not wild-type-like), though of course insufficient (see above). Third, alternating purines and pyrimidines are unnecessary and probably insufficient [it is hard to imagine that AUAUAU, $\Delta G°$ (37) of −1.1 kcal/mol, would be acceptable]. Last, a 100% G/C-rich content might be sufficient (based on data with GGGCCC and GCGCGC).

UGCG261 appeared less functional than GGCC or GUAC (Table 5) on the grounds that UGCG viruses were 80% less infectious than HIV-1_{Lai}. We hypothesize that UGCG is found in 2% of sequenced HIV-1 merely because it is a transition sequence linking CGCG to UGCA via single point-mutations. In contrast, GGCC or GUAC cannot be reached from CGCG or UGCA without forming nonpalindromic transition sequences which are highly deleterious if GGCG of Table 1 is typical. We conclude that if HIV-1 was more evolved, and if available sequences (probably biased toward North American and European isolates) were more representative, the number of extant GGCC and GUAC tetramers might surpass the number of extant UGCG tetramers.

On Stem−Loop B: Generalities. Little is known about the role of the 11 nts tentatively visualized in Figure 1 as stem−loop B. Here we have initiated experiments to estimate the importance of stem−loop B in HIV-1 replication, HIV-1 RNA dimerization, and genomic RNA encapsidation. We have made four notable findings.

First, deletion of the 5′ strand of stem−loop B inhibits viral replication as much as destruction of the kissing-loop hairpin (compare Δ243−247 to Δ248−261 in Table 1). This is consistent with the absolute conservation of CUCGG247 among all HIV-1/SIV$_{cpz}$ strains so far sequenced (2) and suggests an important function for it (see below). Second, Δ243−247 RNA could loose-dimerize very poorly, but only if it contained the 3′ DLS (Table 3). Thus, Δ243−247 has a predominantly indirect influence on RNA dimerization at 30−37 °C: transforming the 3′ DLS into an inhibitor of RNA dimerization. Third, Δ243−247 RNA tight-dimerized as well as HIV-1_{Lai} RNA (compare △ to thick continuous line in Figures 2−4), indicating that Δ243−247 no longer misdirects the 3′ DLS at the higher temperatures used to study tight dimerization. Fourth, Δ243−247 had a moderate effect on genomic RNA encapsidation. This is consistent with studies showing that deleting loop B or replacing its nucleotides by Us reduces genomic RNA packaging 2−3-fold (*5*). We conclude that stem−loop B plays an indirect role in loose RNA dimerization and no role in tight RNA dimerization. We would like to imagine that CUCGG247 plays a significant role both in proviral DNA synthesis and in the dimerization of genomic RNA isolated from viruses (Ni Shen, in progress), thereby accounting for its large impact on viral replication.

Evidence for Stem B Folding in RNAs Starting Upstream of the U5 Region.[8] It has been proposed that formation of stem B might be preempted by the base-pairing of C243 or CGAG277 to nucleotides of the U5 region: GGAC243 and AGGCGAG277 have been respectively base-paired to GUCU115 (*22*) and CUUAAGCCU71 (*23*). Contrary to RNA 178−384 studied by Clever et al. (*21*), our RNAs are theoretically free to adopt these alternative foldings. If the stem B folding of Figure 1 is physiological, then altering its 5′ or 3′ strand should have similar effects. We have deleted the 5′ strand of stem−loop B; Clever et al. (*21*) have replaced the 3′ strand of stem B by an unrelated sequence. Strikingly, Δ243−247 RNA ending at G401 and RNA178−384 with the 3′ strand substitution were monomeric in buffer H at 30−37 °C (see Results; ref *21*). This strongly supports the existence of stem B in RNAs containing an intact 5′ end. Note also that the duplex suggested as an alternative to stem B (*22*) has only 2 or 3 base pairs in SIV$_{cpz}$, subtypes O and U of HIV-1, and in some subtypes C and E of HIV-1; in contrast, stem B always has at least 4 base pairs in all HIV-1/SIV$_{cpz}$ strains (*2, 24, 25*).

The 3′ DLS: A Molecular "Dr. Jekyll and Mr. Hyde" Tuned by the ACS and Stem−Loop B Poles of the KLD. We found that mutations in the two ends of the KLD, namely, the ACS and stem−loop B, can tune the 3′ DLS toward *stimulatory, neutral, or inhibitory* impacts on RNA dimerization. First, the 3′ DLS stimulated loose dimerization of GUAC RNA and stabilized loose dimers of UGCA and UGCG RNAs. Second, it had no effect on the thermostability of AGCU and UUAA RNA loose dimers (RNAs where a positive effect would have been easily visible). Third, it inhibited loose dimerization of Δ243−247 RNA. Fourth, it inhibited tight dimerization of AGCU and UUAA RNAs.

[7] G/C poor palindromic hexanucleotides have predicted free energy changes of duplex formation ranging from −0.7 (AAAUUU) to −5.3 (e.g., UCUAGA) kcal/mol (*27−29*).

[8] The U5 region extends from A98 to G181; it is followed by the primer binding site.

Table 6: Positive (+) and Negative (−) Impacts of the 3′ DLS on HIV-1 RNA Dimerization[a]

mutation in kissing-loop domain	effect of 3′ DLS on loose dimerization	effect of 3′ DLS on tight dimerization yield
GUAC	+[b]	+
UGCA	+[c]	0
UGCG	+[c]	0
GGCC	0	0
CGCG (control)	0	0
AGCU	0	−
UUAA	0	−
Δ243−247	−[d]	0

[a] Figures 2−4 and Tables 3 and 4 should be consulted for details. [b] Higher T_d and higher yield. [c] Higher T_d. [d] Lower yield.

This is summarized in Table 6. Mutations which transformed the 3′ DLS into an inhibitor of dimerization yielded replication defective viruses, while mutations which channeled it toward a positive or neutral impact yielded wild-type-like viruses. This may be more than a coincidence. Molecular models of HIV-1 RNA will need to subtly link together the ACS, stem−loop B, and 3′ DLS poles of the dimerization machinery into a functional whole.

ACKNOWLEDGMENT

We thank Rhona Rosenzweig for the preparation of the typed text.

REFERENCES

1. Coffin, J. (1984) in *RNA tumor viruses* (Weiss, R., Teich, N., Varmus, H., and Coffin, J., Eds.) pp 261−368, Cold Spring Harbor Laboratory Press, Cold Spring Harbor, NY.
2. Laughrea, M., Jetté, L., Mak, J., Kleiman, L., Liang, C., and Wainberg, M. A. (1997). *J. Virol. 71,* 3397−3406.
3. Paillart, J. C., Berthoux, L., Ottmann, M., Darlix, J.-L., Marquet, R., Ehresmann, B., and Ehresmann, C. (1996) *J. Virol. 70,* 8348−8354.
4. Berkhout, B., and Van Wamel, J. L. B. (1996) *J. Virol. 70,* 6723−6732.
5. Clever, J., and Parslow, T. G. (1997) *J. Virol. 71,* 3407−3414.
6. McBride, M. S., and Panganiban, A. T. (1997) *J. Virol. 71,* 2050−2058.
7. Haddrick, M., Lear, A. L., Cann, A. J., and Heaphy, S. (1996) *J. Mol. Biol. 259,* 58−68.
8. Liang, C., Li, X., Quan, Y., Laughrea, M., Kleiman, L., Hiscott, J., and Wainberg, M. A. (1997) *J. Mol. Biol. 272,* 167−177.
9. Li, X., Liang, C., Quan, Y., Chandok, R., Laughrea, M., Parniak, M. A., Kleiman, L., and Wainberg, M. A. (1997) *J. Virol. 71,* 6003−6010.
10. Laughrea, M., and Jetté, L. (1994) *Biochemistry 33,* 13464−13474.
11. Skripkin, Paillart, J.-C., Marquet, R., Ehresmann, B., and Ehresmann, C. (1994) *Proc. Natl. Acad. Sci. U.S.A. 91,* 4945−4949.
12. Laughrea, M., and Jetté, L. (1996) *Biochemistry 35,* 9366−9374.
13. Laughrea, M., and Jetté, L. (1996) *Biochemistry 35,* 1589−1598.
14. Muriaux, D., Fossé, P., and Paoletti, J. (1996) *Biochemistry 35,* 5075−5082.
15. Muriaux, D., De Rocquigny, H., Roques, B.-P., and Paoletti, J. (1996) *J. Biol. Chem. 271,* 33686−33692.
16. Paillart, J.-C., Marquet, R., Skripkin, E., Ehresmann, B., and Ehresmann, C. (1994) *J. Biol. Chem. 269,* 27486−27493.
17. Laughrea, M., and Jetté, L. (1997) *Biochemistry 36,* 9501−9508.
18. Peacock, A. C., and Dingman, C. W. (1967) *Biochemistry 6,* 1818−1827.
19. Sambrook, J., Fritsch, E. F., and Maniatis, T. (1989) *Molecular cloning, a Laboratory Manual,* Cold Spring Harbor Laboratory Press, Cold Spring Harbor, NY.
20. Fu, W., Gorelick, R. J., and Rein, A. (1994) *J. Virol. 68,* 5013−5018.
21. Clever, J. L., Wong, M. L., and Parslow, T. G. (1996) *J. Virol. 70,* 5902−5908.
22. Berkhout, B. (1996) *Prog. Nucleic Acid Res. Mol. Biol. 54,* 1−34.
23. Baudin, F., Marquet, R., Isel, C., Darlix, J.-L., Ehresmann, B., and Ehresmann, C. (1993) *J. Mol. Biol. 229,* 382−397.
24. Gao, F., Robertson, D. L., Morrison, S. G., Hui, H., Craig, S., Decker, J., Fultz, P. N., Girard, M., Shaw, G. M., Hahn, B. H., and Sharp, P. M. (1996) *J. Virol. 70,* 7013−7029.
25. Korber, B., Hahn, B., Foley, B., Mellors, J. W., Leitner, T., Myers, G., McCutchan, F., and Kuiken, C. (1997) *Human Retroviruses and AIDS: a compilation and analysis of nucleic acid and amino acid sequences,* Los Alamos National Laboratory, Los Alamos, NM.
26. Paillart, J. C., Westhof, E., Ehresmann, C., Ehresmann B., and Marquet, R. (1997) *J. Mol. Biol. 270,* 36−49.
27. Freier, S. M., Kierzek, R., Jaeger, J. A., Sugimoto, N., Caruthers, M. H., Neilson, T., and Turner, D. H. (1986) *Proc. Natl. Acad. Sci. U.S.A. 83,* 9373−9377.
28. He, L., Kierzek, R., Santa Lucia, J., Walter, A. E., and Turner, D. H. (1991) *Biochemistry 30,* 11124−11132.
29. Turner, D. H., Sugimoto, N., and Freier, S. M. (1988) *Annu. Rev. Biophys. Biophys. Chem. 17,* 167−192.

BI981728J